Molecular Dynamics Study of the Folding of Hydrophobin SC3 at a Hydrophilic/Hydrophobic Interface

Ronen Zangi,* Marcel L. de Vocht,[†] George T. Robillard,[†‡] and Alan E. Mark*

*Department of Biophysical Chemistry and [†]Department of Biochemistry, University of Groningen, and [‡]Biomade Technology Foundation, Nijenborgh 4, 9747 AG Groningen, The Netherlands

ABSTRACT   Hydrophobins are fungal proteins that self-assemble at hydrophilic/hydrophobic interfaces into amphipathic membranes. These assemblages are extremely stable and posses the remarkable ability to invert the polarity of the surface on which they are adsorbed. Neither the three-dimensional structure of a hydrophobin nor the mechanism by which they function is known. Nevertheless, there are experimental indications that the self-assembled form of the hydrophobins SC3 and EAS at a water/air interface is rich with β-sheet secondary structure. In this paper we report results from molecular dynamics simulations, showing that fully extended SC3 undergoes fast (~100 ns) folding at a water/hexane interface to an elongated planar structure with extensive β-sheet secondary elements. Simulations in each of the bulk solvents result in a mainly unstructured globular protein. The dramatic enhancement in secondary structure, whether kinetic or thermodynamic in origin, highlights the role interfaces between phases with large differences in polarity can have on folding. The partitioning of the residue side-chains to one of the two phases can serve as a strong driving force to initiate secondary structure formation. The interactions of the side-chains with the environment at an interface can also stabilize configurations that otherwise would not occur in a homogenous solution.

INTRODUCTION

Hydrophobins are small fungal proteins (~100 amino acids residues) that self-assemble at hydrophilic/hydrophobic interfaces (e.g., water/air, water/oil, and water/solid-hydrophobic-surface) into amphiphatic membranes. They are responsible for many functions in fungal growth and development, such as the formation of hydrophobic surfaces found in aerial hyphae, spores, and fruiting bodies (Wösten et al., 1994; Talbot et al., 1996; Wessels, 1997; Wösten and Wessels, 1997).

Hydrophobins exhibit interfacial activity and are among the most surface-active biomolecules known. Based on the hydropaty patterns and on the solubility of the assembled membranes, hydrophobins are classified into two classes, I and II (Wessels, 1994). In the class I hydrophobins, the amphipathic membrane is highly insoluble and on the hydrophobic side it is characterized by a rodlet pattern that resembles that of amyloid proteins. Assemblages formed by class II hydrophobins are more soluble and do not form rodlet structures.

SC3, a glycosylated hydrophobin that is secreted by *Schizophyllum commune* (Wessels et al., 1991; Wösten et al., 1993), is currently the most surface-active protein known (with a maximal lowering of the water surface tension from 72 mJ/m^{-2} to 24 mJ/m^{-2}). It is also the most extensively studied hydrophobin to date. SC3 hydrophobin is released into the growth medium in a water-soluble form

that subsequently self-assembles into insoluble films at the water/air interface. SC3 is a class I hydrophobin and is posttranslationally modified with 16 to 22 O-linked mannose residues being attached to the N-terminal part of the peptide chain.

Class I hydrophobins are characterized by a specific hydropathy pattern in their primary sequence and the strict conservation of eight cysteine residues that form four disulfide bridges.

The secondary structure content of soluble and assembled SC3 hydrophobin as inferred from Fourier transform infrared, and circular dichroism (CD) studies (de Vocht et al., 1998) is summarized in Table 1.

The soluble form of SC3 contains on average ~40% β-sheet structure, which increases to 65% on self-assembly. This enhancement of β-sheet structure at the water/air interface plays an important role in the properties of hydrophobins, specifically in the ability to reduce the surface tension and to organize into the characteristic rodlet structure.

The secondary structure content of SC3 at the interface between water and an apolar liquid is not known. However, rodlet formation is observed at a water/oil interface, suggesting that SC3 adopts a primarily β-sheet structure at this interface (Wösten et al., 1994).

No tertiary structure of hydrophobins is available. It has not been possible to obtain high-quality nuclear magnetic resonance spectra of the soluble form of SC3 due to aggregation. It has also not been possible to stabilize the soluble form by the addition of sodium dodecyl sulfate, ethanol or dimethyl sulfoxide. Secondary structure prediction by a profile-fed neural network system predicts that the N-terminal segment before the first cysteine residue (which contains the mannose residues) consists primarily of loop struc-

---

TABLE 1   Percentage of specific secondary structure elements in SC3 as inferred from ATR-FTIR spectroscopy

	α-Helix	β-Sheet	β-Turn	Coil
Soluble	23	41	16	20
Assembly at water/air	16	65	9	10

Data taken from reference (de Vocht et al., 1998).

ture. The remaining part of SC3, the cysteine-rich region, consists of alternating β-sheet and loop structures.

The cysteine-rich region is the region where the enhancement of the β-sheet structure takes place upon assembly at an interface. This is evident from studies on a truncated SC3 in which 26 of the 31 N-terminal amino acids were removed (Fig. 1). Neither the functionality of the protein nor the conformational changes that occur upon assembly were affected. Truncated SC3 is able to self-assemble and to form rodlets. It shows the same degree of surface tension reduction but weaker binding to hydrophilic surfaces (de Vocht et al., 1998).

The origin of the strong interaction between hydrophobins and hydrophobic surfaces is unknown. Protein adsorption is often characterized by a loss of secondary and tertiary structure and may be associated with an increase in entropy of the peptide and enhanced rotational mobility around the polypeptide backbone. In contrast, hydrophobins show an increase in secondary structure upon adsorption indicating that specific conformational changes give rise to the strong hydrophobic adhesive properties.

The water/air interface apparently acts as a catalyst for the formation of rodlets but is not required for stability.

After drying down a solution of SC3 a rodlet layer with a thickness of ~10 nm is obtained. The diameter of a typical 100 amino acid globular protein is ~3 nm. Thus, the rodlets must be comprised of more than one protein layer or the protein must be highly elongated in shape.

Interfacial folding is observed not just in hydrophobins but also in other protein systems such as transmembrane proteins, toxins, antibiotics, and some hormones. Experimental studies have shown that certain naturally occurring (Cornell et al., 1993; Wu et al., 1995; Pérez-Payá et al., 1997; Bernèche et al., 1998), synthetic peptides (Tamm et al., 1989; Takahashi, 1990; Bechinger, 1996; Russell et al., 1998), and fragments of larger proteins (Segrest et al., 1994; Chernomordik et al., 1994; Voglino et al., 1998; Johnson et al., 1998), can readily form amphipathic structures at hydrophilic/hydrophobic interfaces. The initial orientation of the peptides is in general parallel to the interface (Ishiguro et al., 1993; Bechinger et al., 1993, 1998; Wu et al., 1995; Cajal et al., 1996). However, at sufficiently high concentration and/or in the presence of an electric field, some adopt a perpendicular orientation (Wu et al., 1995; Biggin and Sansom, 1996; Lear et al., 1997).

As it is difficult to study the process of adsorption at interfaces in atomic detail experimentally, several groups have turned to molecular dynamics (MD) computer simulation techniques to investigate interfacial folding. Chipot and Pohorille (1998b) showed in a simulation study of an undecamer of poly-L-leucine at a water/hexane interface that when placed initially on the water side in a random coil conformation, the peptide translocated toward the hexane phase and underwent interfacial folding into an α-helix. The
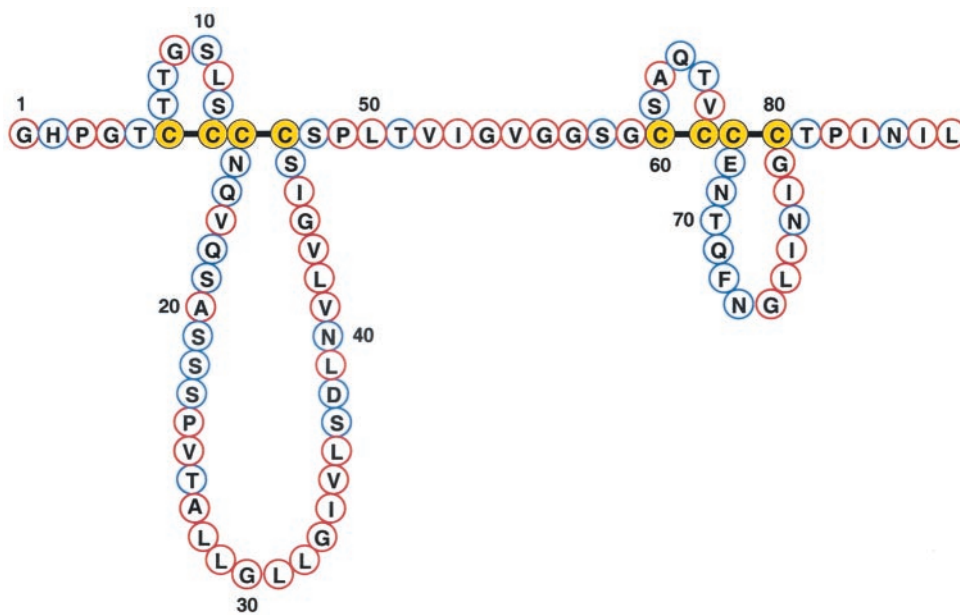

FIGURE 1   Primary structure of truncated SC3 showing the four loops formed by the four disulfide bridges. Cysteine residues are yellow. Hydrophilic and hydrophobic residues are blue and red, respectively.

helical peptide was largely buried in hexane yet remained adsorbed at the interface with a parallel orientation. The rapid coil to helix transition, which occurred within 36 ns, suggested that at interfaces elements of secondary structure may form before slower, long range tertiary contacts are made.

The placement of an amphipathic peptide or protein at an interface between a hydrophilic and a hydrophobic phase (which in effect represents an external electric field) introduces an additional parameter that can determine the nature of the free energy surface and its minimum. Amino acid residues of the peptide or protein will partition into the respective phases according to their hydrophobicity. This will preorganize the structure in solution leading to rapid secondary structure formation. There are indications that in some cases the optimum conformation is insensitive to the nature of the hydrophobic phase. Some amphipathic peptides adopt the same secondary structure at water/membrane, water/alkane, and water/air interfaces (DeGrado and Lear, 1985; Chung et al., 1992; Blondelle et al., 1995).

Although the partitioning of residues into one of the phases can initiate secondary structure formation, transitions between different amphipathic structures at an interface could require the surmounting of high free energy barriers. Nonoptimized folded structures with a satisfactory partitioning of the residues may represent local minimum on the free energy surface and impede folding (Chipot et al., 1999).

In this paper, MD simulation techniques are used to study the initial stages of folding of hydrophobin SC3 at a water/hexane interface. The behavior of SC3 in bulk water and bulk hexane is also investigated for comparison. We find that fully extended SC3 undergoes rapid folding at a water/hexane interface to a structure with extensive β-sheet content. Simulations in each of the bulk phases result in a mainly unstructured globular protein. The enhancement of secondary structure, whether kinetically or thermodynamically determined, highlights the role interfaces with a large difference in polarity can have in catalyzing folding. The partitioning of the residue side-chains between the two phases provides a strong driving force to initiate secondary structure formation. Furthermore, the interaction of given side-chains within a hydrophobic or hydrophilic environment can initially stabilize the creation of structural elements that might otherwise not occur in a homogenous solution.

MATERIALS AND METHODS

The MD simulations were preformed using the GROMACS package version 2.0 (Berendsen et al., 1995; van der Spoel et al., 1999) with the GROMOS96 (43A2) force field (van Gunsteren et al., 1996). SC3 was simulated in three different environments: a water/hexane interface, bulk water, and bulk hexane. Water was described by the simple point charge (SPC) model (Berend-sen et al., 1981). The hexane model was taken from the GROMOS96 force field version 43A2 in which the equilibrium distri-

bution of dihedral angles in alkanes is reproduced better then in previously published force field versions (Schuler and van Gunsteren, 2000).

To maintain the system at a constant temperature of 300 K, a Berendsen thermostat (Berendsen et al., 1984) was applied using a coupling time of 0.1 ps. The pressure was maintained by coupling to a reference pressure of 1 bar. A coupling time of 1.0 ps was used for the simulations at the interface and in bulk water, whereas a coupling constant of 2.0 ps was used for the simulation in bulk hexane (Berendsen et al., 1984). The values of the isothermal compressibility were set to 10.6×10^{-5}, 4.5×10^{-5}, 16.7×10^{-5} bar^{-1} for water/hexane, water and hexane simulations, respectively. For the evaluation of the nonbonded interactions a twin range cutoff of 0.9 and 1.4 nm was used. Interactions within the shorter cutoff were updated every step, whereas interactions within the longer cutoff were updated every five steps. For the systems that contained water, the time step used was 0.002 ps. However, because the GROMOS96 force field uses a united atom model for CH_2 and for CH_3 groups a larger time step was used for the simulations in bulk hexane. After 14 ns from the point the sulfur-sulfur (S-S) bonds were formed, the time step was increased from 0.002 to 0.004 ps. At the same time the mass of the polar hydrogen atoms within the protein, which were treated explicitly, was increased to 4 amu. The increased mass of the hydrogen was subtracted from the mass of the heavy atom to which the hydrogen was bonded leaving the total mass unchanged. The overall result is the removal of high frequency vibrational motion involving the hydrogen atoms allowing an increase of the integration time step (Feenstra et al., 1999).

Water bond distances and angles were constrained using the SETTLE algorithm (Miyamoto and Kollman, 1992), whereas the hexane and the protein bond distances were constrained using the SHAKE algorithm (Ryckaert et al., 1977) with a geometric tolerance of 1×10^{-4}.

The system simulated was that of an 86 amino acid truncated form of SC3, the same as that used in the corresponding experimental studies. In this form of SC3, 29 N-terminal residues of the native SC3 (up to two amino acids before the first cysteine) were removed and substituted by the sequence Gly-His-Pro (see Fig. 1). This three amino acid sequence is characteristic of many hydrophobins at this position. The N and the C termini were protonated and deprotonated, respectively. The negative charges carried by the residues Asp-38 and Glu-68 resulted in a total charge of $-2e$.

The starting structure of the protein in the three simulations was a fully extended conformation of truncated SC3 constructed using the program WHATIF (Vriend, 1990). In the simulation of the water/hexane interface the extended protein was aligned on the interface.

The simulation cell was a rectangular periodic box with the minimum distance between the protein and the box walls set to 0.75 nm, so that the protein did not directly interact with its own periodic image given the cutoff. The box dimensions were changed several times during the simulations. This was necessary because the protein underwent very large changes in shape (especially at the beginning) and for reasons of efficiency as initially large amounts of solvent were required to solvate the extended structures ($\sim$79,000 atoms in the case of bulk water). The extended conformation enforced a single long axis on the simulation box. As the protein collapsed the other two axes had to be increased to prevent the protein being restricted in any direction. To change the box dimensions, the protein configuration and the maximum possible volume of solvent around it (as determined by the new box dimensions) were kept. A new region of preequilibrated solvent molecules was then added to the extended direction. In the water/hexane simulations, the length of the axis perpendicular to the interface was held constant when changing the box size. The length of this axis fluctuated (due to the pressure coupling) around 4.7 nm throughout the simulation.

To form the four disulfide bridges starting from the extended conformation of the protein, distance constraints between the pairs of sulfur atoms that form disulfide bridges were imposed. A coupling parameter λ was used to gradually reduced the constraint distance from that in the fully extended conformation (λ is 0) to an S-S distance of 0.21 nm (λ is 1). During this process, each of the S-S distances were decreased at each step

TABLE 2 Details of the procedures used to conduct the simulations in the three environments

	Simulation of SC3 in:		
	Water/hexane	Water	Hexane
Initial # of water molecules	7972	25,990	–
Initial # of hexane molecules	1436	–	6780
Number of steps of energy minimization	30	30	530
Relaxation time before S-S (ns)	2.4	–	–
Time of S-S (ps)	400	400	200
Relaxation time after S-S (ns)	135	100	100

S-S denotes the disulfide-bridge forming process.

by a distance corresponding to $\Delta\lambda = 1 \times 10^{-5}$. Once the four S-S distances reached 0.21 nm the distance restraint was replaced by a bond constraint between the sulfur atoms of 0.204 nm as given in the force field used. The process of S-S bond formation was performed separately in each of the three different environments. In the simulations at the interface and in water the process was split into two stages to allow for a reduction in the size of the system.

The degree of amphipathy of the protein was estimated from its mean structural hydrophobic moment (Eisenberg et al., 1982), $\langle \vec{\mu}_H \rangle$,

$$\langle \vec{\mu}_H \rangle = \frac{1}{N} \sum_{i=1}^{N} H_i \times \vec{S}_i \qquad (1)$$

in which N denotes the number of amino acid residues in the protein, H_i is the hydrophobicity of residue i and $\vec{S}_i$ is the unit vector pointing from the α-carbon atom of the ith residue to the center of mass of its side-chain. The values for the hydrophobicities, H_i, were taken from Wolfenden et al. (1981). Because in glycine the side chain hydrogens are incorporated into the α-carbon, which is treated as a united atom, the contribution of glycine residues to the hydrophobic moment was not considered.

The analysis of the secondary structure elements was based on the DSSP (define secondary structure of proteins) definitions (Kabsch and Sander, 1983). The figures of the protein, and thereby the secondary structure assignment shown in the figures, were generated using the visualization package MOLMOL (Koradi et al., 1996).

Details regarding the simulations in the three environments are given in Table 2. Note that in the simulation at the water/hexane interface the system was relaxed for 2.4 ns before the process of disulfide bridge formation was initiated. This was to allow the orientation of the residue side-chains in the extended conformation (initially placed arbitrarily) to relax and insert into their preferred phase. The time required for the side-chains to reorient was in the order of a few hundred picoseconds.

A second simulation of truncated SC3 at the water/hexane interface was performed for 51 ns. The starting conformation was taken from the first simulation at the interface after the formation of the sulfur bonds (i.e., at $t = 0$) but with new random velocities. This simulation is labeled water/hexane-2.

All simulations were performed on a PentiumIII based linux cluster. The 135-ns trajectory at the interface required approximately the equivalence of five months processing time on a 866 MHz dual processor node.

RESULTS

In the initial stage of the relaxation process, after the S-S bonds were formed, the peptide chain contracted rapidly (within picoseconds) as the linear conformation of the segment of peptide between the second and third loops, which was unaffected by the formation of the disulfide bridges, is highly unfavorable. Following this initial phase, the system
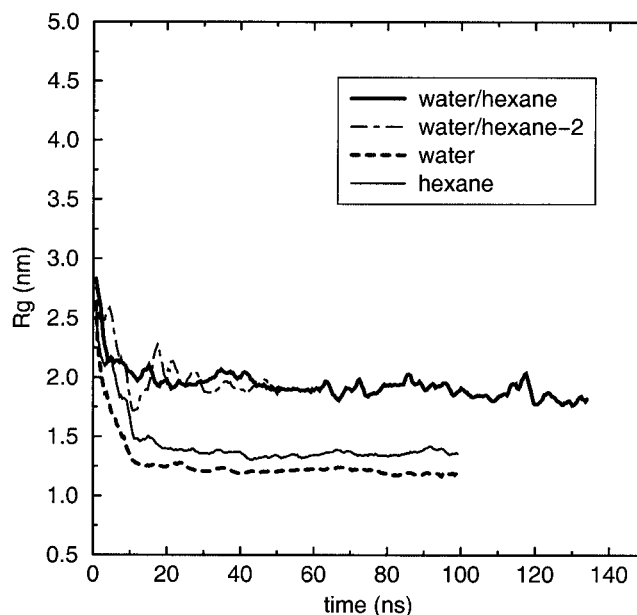

FIGURE 2 Radius of gyration (nanometers) of SC3 as a function of time at the water/hexane interface, in water and in hexane. The zero time indicates the point at which the disulfide bridges were formed. The values were calculated every 400 ps and averaged over a window of five adjacent points.

continued to collapse but at a slower rate (nanoseconds). The radius of gyration of SC3 as a function of time in each of the three environments is shown in Fig. 2.

The radius of gyration in bulk water and bulk hexane was 1.2 and 1.4 nm, respectively. At the interface, the value of the radius of gyration was 1.9 nm. This reflects the large value of the interface-plane component as is also apparent from inspection of the final structure.

The structures of SC3 at selected points along each trajectory are plotted in Figs. 3, 4, and 5.

The structure formed at the interface is essentially planar with the peptide lying along the interfacial plane throughout the trajectory. In contrast the structures in the bulk solvents are globular. There is a clear enhancement of secondary structure formation at the interface compared with that in the bulk solvents. This is mainly in a form of β-sheet, although there is a small region (5–7 residues long) with α-helical structure. A plot of the secondary structure, defined using the DSSP algorithm, as a function of time is shown in Fig. 6.

The formation of β-sheets at the interface was observed to be a dynamic process especially at the initial stage of the trajectory. In few cases small segments folded then unfolded only to later refold with the same residues or with others. However, the number of such events decreases as the folding of SC3 progresses. The addition of the third and the fourth strands to the two-stranded β-sheet segment initially formed is partialy sequential.
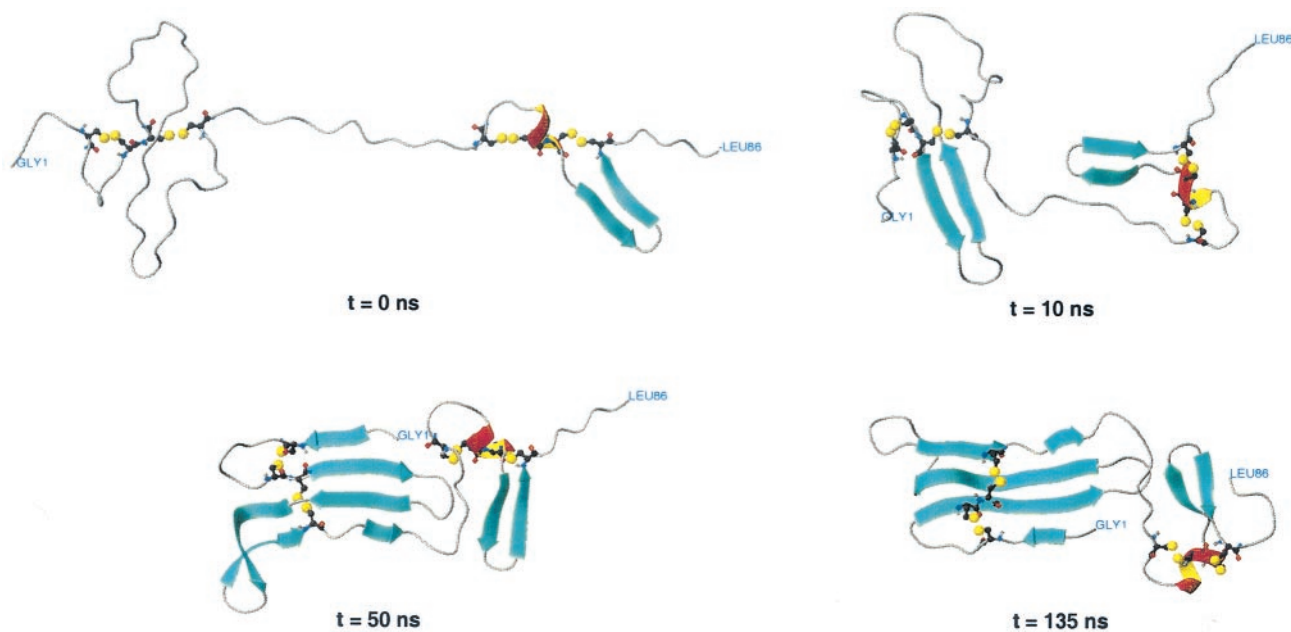
FIGURE 3 Structures of SC3 from the simulation at the water/hexane after 0, 10, 50, and 135 ns. The sulfur atoms in the cysteine residues are shown in yellow.

Selected structures from the second simulation at the water/hexane interface as well as the DSSP plot are shown in Fig. 7.

The extended starting conformation used in all the simulations is highly unstable. The simulations give rise to nonequilibrium trajectories and large variations in the structure of the protein as a function of time (especially in the initial part of the trajectory) are observed. This makes any statistical analysis of the trajectories problematic and requires a somewhat arbitrary choice of when the system has "equilibrated." In the analysis that follows, the first 50 ns were excluded in the case of the longer trajectories in each of the three environments, whereas for the shorter simulation at the interface, water/hexane-2, only the first 25 ns
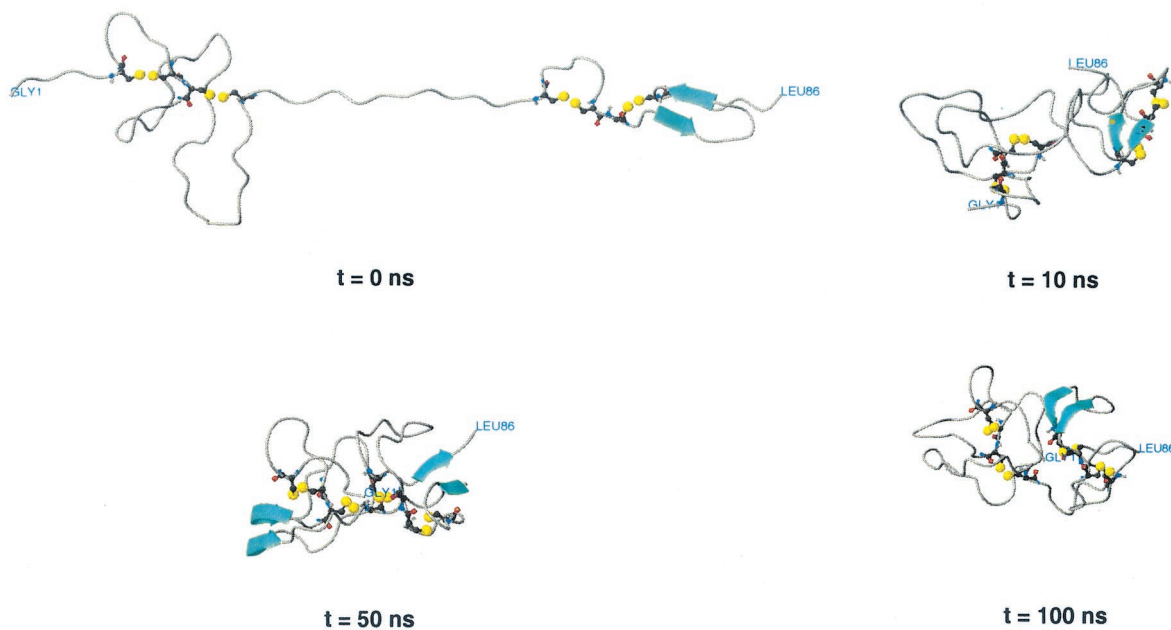

FIGURE 4 Structures of SC3 from the simulation in water after 0, 10, 50, and 100 ns. The sulfur atoms in the cysteine residues are shown in yellow.
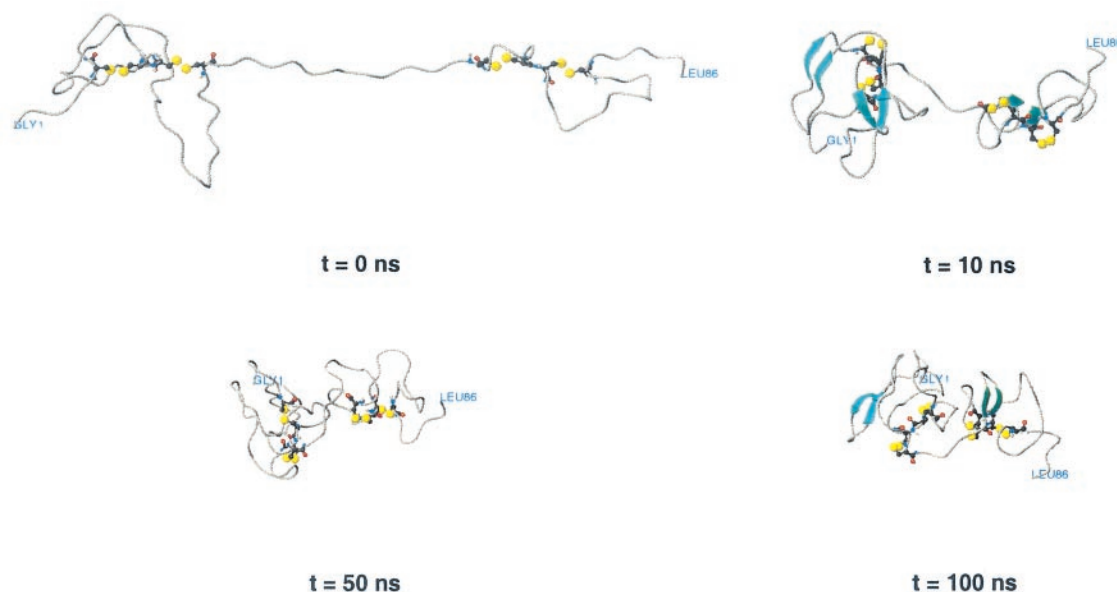
FIGURE 5 Structures of SC3 from the simulation in hexane after 0, 10, 50, and 100 ns. The sulfur atoms in the cysteine residues are shown in yellow.

were discarded. The average secondary structure content for each simulation is summarized in Table 3.

The major difference between the two simulations at the interface is the lower percentage of β-sheet structure and the absence of α-helix in the second simulation. However, the same general mechanism of folding at the interface, that of an essentially quasi two-dimensional system yielding a planar folded structure with the very rapid formation of β-sheet was found in both simulations.

The hydrophobic moment (Fig. 8) and the solvent accessible surface area of the protein were calculated from the trajectories and are summarized in Table 4.

As expected the alignment of the side-chains leads to a more amphipathic structure in the simulation at the interface then in either of the two bulk phases. The value of $\langle \vec{\mu}_H \rangle$ at the interface is at least twice as high as the value obtained in water or in hexane.

Truncated SC3 contains 41 hydrophilic and 45 hydrophobic residues. Therefore, it is reasonable to expect that, qualitatively, the behavior of the collapsed structure in water and in hexane would be similar (although different residues would be exposed to solvent) and that the value of the hydrophobic moment would be comparable. This is the case even though the radius of gyration and the solvent accessible surface area are higher in hexane.

To determine the time scale on which side-chains orientate toward their preferred solvent, and to obtain values of $\langle \vec{\mu}_H \rangle$ when no constraints on the sulfur atoms were imposed, a series of short (2 ns) simulations were performed from a fully extended conformation. The simulations were conducted in the three environments and during the 2 ns simulated neither the collapse of the structure nor any second-

ary structure formation was observed. The orientation of side-chains is relatively fast ($\sim$200 ps) and the value of $\langle \vec{\mu}_H \rangle$ averaged over the last 1 ns is 0.95, 0.40, and 0.27 for the simulations at the interface, in water, and in hexane, respectively. Thus, there is a marked decrease in the value of $\langle \vec{\mu}_H \rangle$ at the interface as the protein folds and attains secondary structure. The average value of the hydrophobic moment in the second simulation at the interface is higher than in the longer simulation. This is to be expected as the percentage of β-sheet is smaller and more residues are free to orientate toward their preferred phase.

To test the tendency of SC3 to reside at the interface, two simulations in which SC3 was placed in the bulk phases but close to the interface were performed. In the first simulation, the peptide was placed in the water phase, and in the second, the peptide was placed in the corresponding manner but in the hexane phase. In both cases, the starting conformation was taken from the extended simulation at the water hexane interface (after 135 ns). Each system was simulated for 4 ns. The behavior of the protein with respect to the interface in the two simulations was very similar. Within a few hundred picoseconds the protein had fully readsorbed on the interface. Figs. 9 and 10 show the initial position of SC3 with respect to the interface as well as the position after 700 ps from the simulations with SC3 starting in water and in hexane, respectively. The time-scale for the migration to the interface and the final interfacial position were comparable in both cases.

Averages of the energy components (Lennard-Jones and Coulomb) were calculated for the interactions inside the protein and for the interactions between the protein and the solvent. The results are shown in Table 5.
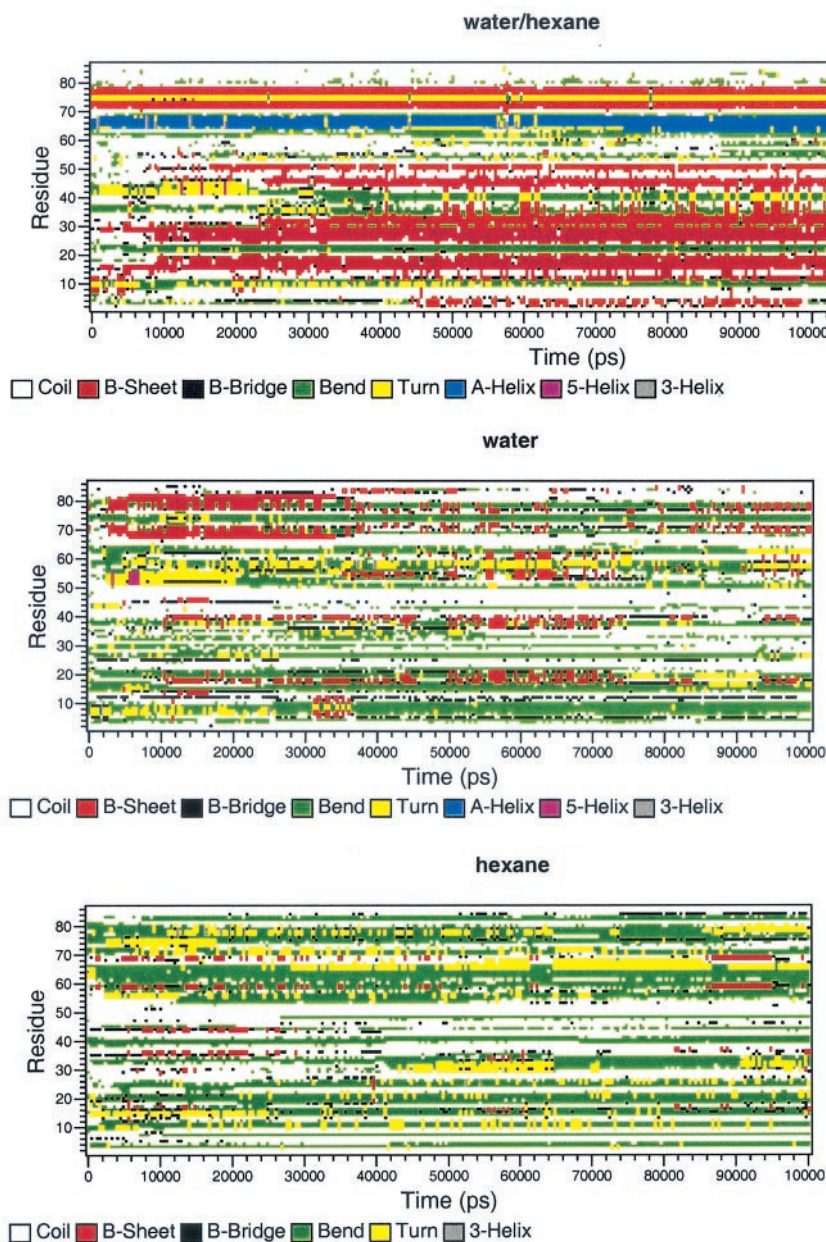
FIGURE 6 Secondary structure assignment of the protein (DSSP) as a function of time for the simulations in the three environments.

The strongest intraprotein interactions occur when the protein is solvated in hexane. As hexane is uncharged, electrostatic interactions act only between atoms within the protein and it is most likely that electrostatic interactions drive the collapse of the protein in this solvent. Surprisingly, the value of the protein-protein interaction energy is slightly higher in the simulation in water than at the water/hexane interface. The primary contribution to the protein-protein electrostatic interaction at the interface is due to the formation of backbone-backbone hydrogen bonds within elements of β-sheet. In water, little regular secondary structure has formed. Nevertheless, the overall intraprotein electrostatic

interaction is comparable with that on the interface. The main difference is the stronger Lennard-Jones interactions, a result of adopting a compact globular structure enforced by the hydrophilic surroundings. The weaker Lennard-Jones interactions within the protein at the water/hexane interface are compensated by interactions between the protein and the solvent. Summing all contributions, the total energy inside the protein and of the protein with the solvent is slightly more favorable in water simulation than at the interface. However, as the energetic (or enthalpic) contribution to the overall free energy of the system for the protein at the interface includes both interactions that involve the protein
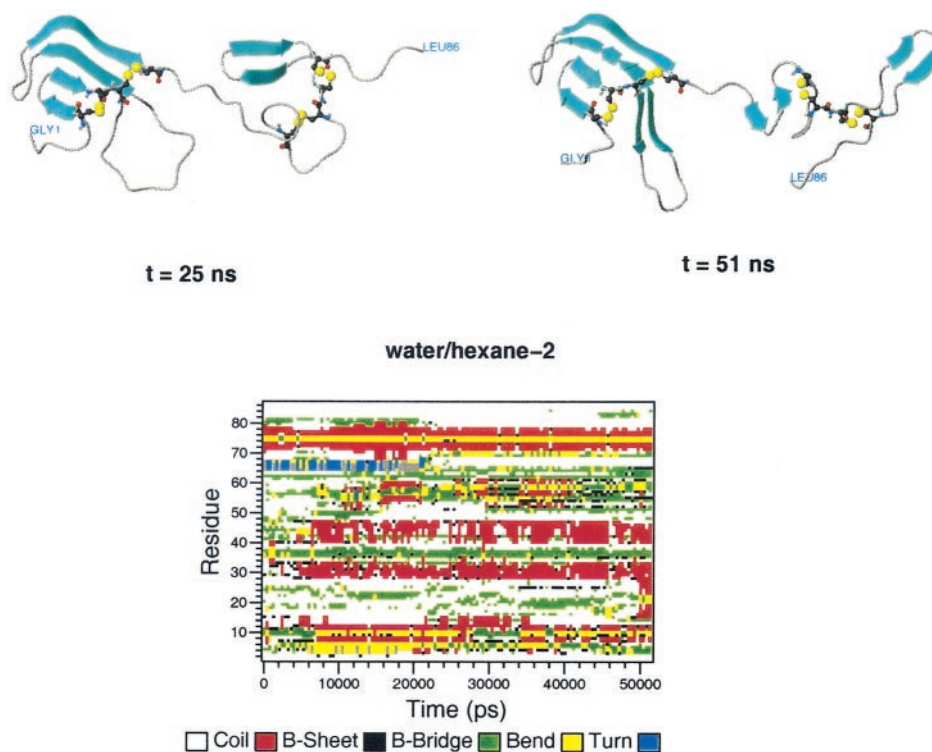
FIGURE 7   Structures of SC3 from the second simulation at the water/hexane interface after 25 and 51 ns. In the lower panel the DSSP plot is drawn.

(intraprotein interactions and interactions with solvent) and interactions between solvent molecules, it is not possible to judge which state should be more stable based on these considerations alone. The entropic contributions to the binding of SC3 at the interface are difficult to assess. The translational entropy in one dimension and the rotational entropy around two axes is lost when the protein is adsorbed onto the interface. The configurational entropy of the backbone on the interface is likely to differ significantly from that in the bulk solvents reflecting the different folded structures in those environments. The dominant effect is, however, most likely to be the gain in water enthalpy when the protein adsorb to the interface as a large area of hydrophobic surface (protein + hexane) is buried.

DISCUSSION

The simulations carried out in this study were designed to capture prominent trends in the folding of SC3 at a water/

hexane interface as compared with the folding in the two bulk phases. As folding, in general, is a process that is characterized by time scales much longer than that which can be currently reached in simulations, the processes the simulations describe can plausibly only constitute the ear-
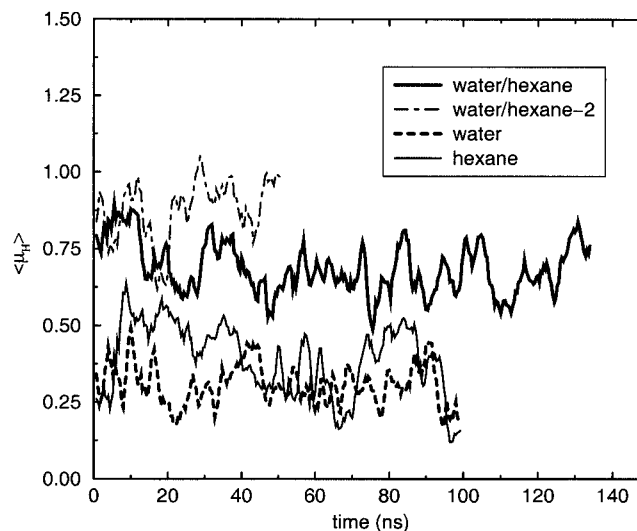

FIGURE 8   Hydrophobic moment of SC3, as defined in Eq. 1, as a function of time from the simulations at the interface and in the bulk solvents. The values were calculated every 400 ps and averaged over a window of five adjacent points.

TABLE 3   **Percentage of secondary structure in SC3 from the simulations at the interface and in the bulk solvents**

Solvents	α-Helix	β-Sheet	β-Bridge	β-Turn	Bend	Coil
Water/hexane	6	36	2	5	19	32
Water/hexane-2	0	26	5	8	20	41
Water	0	7	6	4	33	50
Hexane	1	1	3	10	43	42

TABLE 4 Solvent accessible surface area (A_{sa}), the radius of gyration (R_g), and the structural hydrophobic moment, $\langle \vec{\mu}_H \rangle$, of the protein at the water/hexane interface, in water, and in hexane

Solvent	A_{sa} (nm^2)	R_g (nm)	$\langle \vec{\mu}_H \rangle$
Water/hexane	38	1.9	0.67
Water/hexane-2	39	1.9	0.93
Water	27	1.2	0.30
Hexane	35	1.4	0.35

liest events in the mechanism of folding. It is not known to what degree the structures generated are related to the true structures, as these are yet to be determined experimentally. There are also other limitations to the study. The computational resources required were considerable and although a second simulation at the interface was performed for 50 ns the statistics are limited. In addition, the force field used has been parameterized for use in aqueous solution and may not
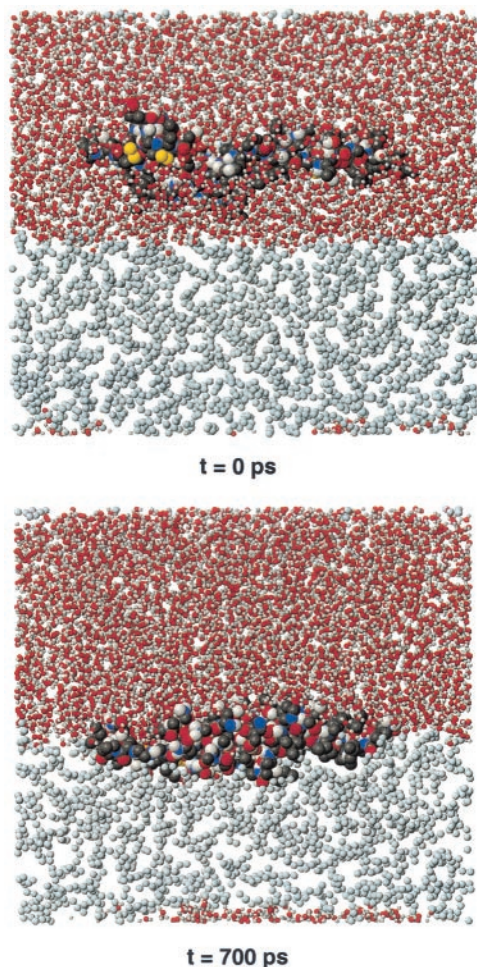

t = 0 ps

t = 700 ps

FIGURE 9 Migration of SC3 from the water phase to the interface. For clarity, only a 2.7-nm slice around the protein is shown. The oxygen atoms of the water molecules are colored red, whereas the atoms of hexane are colored gray.
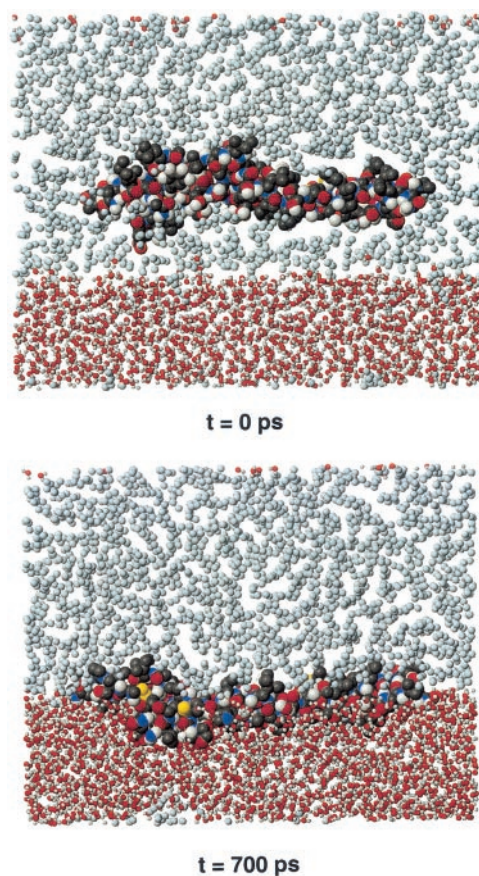
t = 0 ps

t = 700 ps

FIGURE 10 Migration of SC3 from the hexane phase to the interface. For clarity, only a 2.7-nm slice around the protein is shown. The oxygen atoms of water are colored red, whereas the atoms of hexane are colored gray.

correctly reproduce the partitioning behavior of individual amino acids. Thus, the simulations and analysis, although suggestive, should be treated with an appropriate degree of caution.

Neither truncated SC3 nor any part of this segment exhibited any tendency to move into either of the two bulk phases during the 135-ns simulation. When placed close to the interface, in either of the two phases, the peptide quickly (within a few hundred picoseconds) readsorbed onto the interface. This indicates that monomeric SC3 is interfacially active and suggests that the migration of monomeric SC3 to the interface may be the initial step in the process of self-assembly.

Interfacial activity is a phenomenon common to many solutes. It is observed experimentally (Baber et al., 1995; North and Cafiso, 1997; Xu and Tang, 1997) and has also been studied theoretically (Chipot et al., 1997; Pohorille et al., 1997) for amphipathic solutes. By examining small uncharged molecules that possess a permanent dipole moment, Pohorille and Wilson (1996) proposed that interfacial activity results from a balance between two opposing con-

TABLE 5 Lennard-Jones and Coulomb interaction energies (KJ/mol) for the simulations of SC3 in the three environments

Interaction type	Water/hexane			Water/hexane-2			Water			Hexane		
	p-p	p-w	p-h	p-p	p-w	p-h	p-p	p-w	p-h	p-p	p-w	p-h
Coulomb	−2711 (169)	−4250 (435)	–	−2826 (257)	−4135 (361)	–	−2667 (220)	−4981 (327)	–	−4278 (83)	–	–
Lennard-Jones	−2111 (28)	−483 (128)	−1352 (92)	−2040 (49)	−519 (63)	−1377 (67)	−2529 (106)	−1050 (59)	–	−2224 (35)	−2113 (32)	
Total	−4822	−4733	−1352	−4866	−4654	−1377	−5196	−6031	−1377	−6502	−2113	−2113

Abbreviations: p, protein; w, water; h, hexane.
The numbers in the parentheses are the values of the root mean square deviations.

tributions, 1) that the loss of free energy associated with cavity formation is lower in the nonpolar phase, and 2) that the gain from electrostatic solute-solvent interactions is larger in water. In the case of SC3 we infer that the strong electrostatic interaction between the water molecules, leading to a high free energy cost for cavity formation, is a major factor contributing to the free energy minimum at the interface. The accumulation at interfaces has also been reported for terminally blocked amino acids and for short amphiphilic or amphipathic peptides at water/hexane (Pohorille and Wilson, 1993; Chipot and Pohorille, 1997, 1998a), water/membrane (Kaiser and Kezdy, 1987; Jacobs and White, 1989; Brown and Huestis, 1993; Pohorille and Wilson, 1994; Damodaran et al., 1995; Blondelle et al., 1995), and water/air (Cornut et al., 1996) interfaces.

In the present study, secondary structure formation (mostly β-sheet) occurred much more rapidly when the peptide was allowed to fold at the interface than in bulk solvent. Clearly, the coexistence of two phases with different polarity provides a driving force that enhances secondary structure formation. Hydrophobins are amphiphatic with alternating segments (1–10 amino acids) of hydrophilic/hydrophobic residues. The forces acting on the side-chains due the solvent molecules in each phase creates a tendency for the hydrophilic residues to migrate toward the water and the hydrophobic residues to migrate toward the hexane. Because the alternating hydrophilic/hydrophobic segments are small, the effect is to restrict the sampling of conformational space. In some cases, the local structure formed by the motion of the side-chains toward one of the two phases serves as an initial nucleus for secondary structure formation. The folding process becomes quasi two-dimensional, yielding a planar conformation of the folded protein.

In the simulations, folded SC3 at the water/hexane interface is planar as opposed to globular in water. The number of short-range inter-protein interactions is, therefore, higher in the globular fold. The similarity in the protein-protein interaction energy in those two cases is possible only due to the extensive hydrogen bonding network formed in the β-sheet arrangement at the interface. This secondary structure enhancement defines a disorder→order transition that is also found in proteins other than hydrophobins.

In a previous computational study of interfacial folding involving an undecamer peptide consisting of a sequence of Leu and Gln residues capable of forming an amphipathic α-helix, it was shown that if the peptide was placed on the water side in a nonamphipathic β-sheet conformation, the peptide would still migrate to the water/hexane interface and adopt a nonhelical amphipathic conformation with nearly optimal amphipathy (Chipot et al., 1999). Almost no nonamphipathic conformations were observed at the interface. Interfacial folding most likely goes through a series of amphipathic intermediates. In the present study, in addition to the secondary structure enhancement, SC3 at the interface is also more amphipathic than the folded globular structures

in water or in hexane. This again suggests a kinetic and/or thermodynamic relationship between amphipathy and folding.

The disorder→order transition, upon moving from a bulk phase to the interface, observed in the simulations of SC3 is also observed experimentally (see Table 1). The effect has been reported to be even more pronounced in another class I hydrophobin, EAS, from the ascomycete *Neurospora crassa* (Mackay et al., 2001). Mackay et al. showed through analysis of NOESY spectra that in aqueous solution EAS is monomeric and essentially unstructured except for a small region of three-stranded antiparallel β-sheet that is probably stabilized by the four disulfide bridges. CD spectra, however, revealed a dramatic increase of β-sheet structure upon self-assembly at an interface.

The simulations in water show only qualitative agreement with the experimental estimates of secondary structure content. The amount of α-helix structure shows the largest discrepancy. A comparison between the secondary structure content inferred experimentally and that found in the simulation at the interface is not straightforward. The experimental results correspond to a fully aggregated assembly of proteins that strongly interact with each other. This introduces considerable uncertainty. Nevertheless, the enhancement of β-sheet structure at the interface, in comparison with the structure in aqueous solution in the simulations is clear.

In an idealized minimum energy configuration of a protein at a water/hexane interface it is expected that all hydrophilic side-chains would point toward the water and all hydrophobic side-chains would point toward the hexane. At the same time, to optimize the intramolecular energy the peptide must adopt a β-sheet structure with the formation of interbackbone hydrogen bonds. If, however, the primary sequence does not consist of alternating hydrophilic and hydrophobic residues both criteria cannot be satisfied simultaneously. The β-sheet conformation forces mismatches between the type of the side-chain and the phase into which it projects. In the case of SC3 there are 19 of the possible 86 such mismatches in the extended simulation. This explains the smaller value of $\langle \vec{\mu}_H \rangle$ at the interface in the fully folded protein as compared with that of the extended structure and also to that of the second shorter simulation in which less β-sheet has formed. These mismatches may, nevertheless, play a role in driving the aggregation of SC3 hydrophobin into rodlets.

The simulation of the monomeric form of SC3 at a hydrophobic/hydrophilic interface has allowed us to identify the effects of this unique environment on the folding of a protein evolved naturally to be interfacially active. The actual mechanism of hydrophobin folding and self-assembly is not known. The investigation of interfacial assembly in atomic detail by experimental means is still intractable. It well may be that the existence of an interface is needed to initiate or facilitate conformational rearrangements associated with other aggregating or fibril forming proteins (Schladitz et al., 1999). In SC3 the conformational rearrangements needed to initiate self-assembly most likely involve β-sheet formation driven by the two-dimensional interface. Nevertheless, it is possible that the parallel to the interface configuration of the monomeric SC3, found in this simulation is only transitory and that the final orientation of fully assembled SC3 polymer is perpendicular to the interface as occurs in the self-assembly of Langmuir monolayers at an air/water interface. The elongated rodlike molecules of which such monolayers can be formed posses a hydrophilic head and a hydrocarbon tail. At low concentration where there is a high surface area per molecule, the system is best described by a gas-like phase where the position of each molecule is at the air/water interface with a parallel orientation of their long axis. As the concentration is increased the system undergoes a phase transition. The condensed phase is characterized by strong interactions between the molecules the orientation of which is perpendicular to the interface with the polar head groups pointing to the water and the hydrophobic tail facing the air (Langmuir, 1933; Stenhagen, 1955).

The folded states of peptides and proteins are determined by a delicate balance between many factors that characterize the thermodynamics of the system. The introduction of an interface can greatly effect the kinetics and mechanism of the folding process. This clearly is one role of chaperones. Amphipathic proteins can be driven rapidly toward their folded state. Hydrophobins have evolved to function only at hydrophilic/hydrophobic interfaces. They have been selected to remain unstructured in other environments. As such they not only have interesting technological properties but also have the potential to teach us more in regard to how and why proteins fold.

REFERENCES

Baber, J., J. F. Ellena, and D. S. Cafiso. 1995. Distribution of general anesthetics in phospholipid bilayers determined using ^{2}H NMR and ^{1}H-^{1}H NOE spectroscopy. *Biochemistry.* 34:6533–6539.

Bechinger, B. 1996. Towards membrane protein design: pH-sensitive topology of histidine-containing polypeptides. *J. Mol. Biol.* 263:768–775.

Bechinger, B., M. Zasloff, and S. J. Opella. 1993. Structure and orientation of the antibiotic peptide magainin in membranes by solid-state nuclear magnetic resonance spectroscopy. *Prot. Sci.* 2:2077–2084.

Bechinger, B., M. Zasloff, and S. J. Opella. 1998. Structure and dynamics of the antibiotic peptide PGLa in membranes by solution and solid-state nuclear magnetic resonance spectroscopy. *Biophys. J.* 74:981–987.

Berendsen, H. J. C., J. P. M. Postma, W. F. van Gunsteren, A. DiNola, and J. R. Haak. 1984. Molecular dynamics with coupling to an external bath. *J. Chem. Phys.* 81:3684–3690.

Berendsen, H. J. C., J. P. M. Postma, W. F. van Gunsteren, and J. Hermans. 1981. Interaction models for water in relation to protein hydration. *In*

Intermolecular Forces. B. Pullman, editor. D. Reidel Publishing Company, Dordrecht, The Netherlands 331–342.

Berendsen, H. J. C., D. van der Spoel, and R. van Drunen. 1995. GROMACS: a message-passing parallel molecular dynamics implementation. *Comp. Phys. Commun.* 91:43–56.

Bernèche, S., M. Nina, and B. Roux. 1998. Molecular dynamics simulation of melittin in a dimyristoylphosphatidylcholine bilayer membrane. *Biophys. J.* 75:1603–1618.

Biggin, P. C., and M. S. Sansom. 1996. Simulation of voltage-dependent interactions of α-helical peptides with lipid bilayers. *Biophys. Chem.* 60:99–110.

Blondelle, S. E., J. M. Ostreh, R. A. Houghten, and E. Pérez-Payá. 1995. Induced conformational states of amphipathic peptides in aqueous/lipid environments. *Biophys. J.* 68:351–359.

Brown, J. W., and W. H. Huestis. 1993. Structure and orientation of a bilayer-bound model tripeptide: a ^{1}H NMR study. *J. Phys. Chem.* 97:2967–2973.

Cajal, Y., F. Rabanal, M. A. Alsina, and F. Reig. 1996. A fluorescence and CD study on the interaction of synthetic lipophilic hepatitis B virus preS(120–145) peptide analogues with phospholipid vesicles. *Biopolymers.* 38:607–618.

Chernomordik, L., A. N. Chanturiya, E. Suss-Toby, E. Nora, and J. Zimmer berg. 1994. An amphipathic peptide from the C-terminal region of the human immunodeficiency virus envelope glycoprotein causes pore formation in membranes. *J. Viriol.* 68:7115–7123.

Chipot, C., B. Maigret, and A. Pohorille. 1999. Early events in the folding of an amphipathic peptide: a multinanosecond molcular dynamics study. *Proteins Struct. Funct. Gen.* 36:383–399.

Chipot, C., and A. Pohorille. 1997. Structure and dynamics of small peptides at aqueous interfaces a multi-nanosecond molecular dynamics study. *J. Mol. Struct. (THEOCHEM).* 398/399:529–535.

Chipot, C., and A. Pohorille. 1998a. Conformational equilibria of terminally blocked single amino acids at the water-hexane interface: a molecular dynamics study. *J. Phys. Chem. B.* 102:281–290.

Chipot, C., and A. Pohorille. 1998b. Folding and translocation of the undecamer of poly-L-leucine across the water-hexane interface. a molecular dynamics study. *J. Am. Chem. Soc.* 120:11912–11924.

Chipot, C., M. A. Wilson, and A. Pohorille. 1997. Interactions of anesthetics with the water-hexane interface: a molecular dynamics study. *J. Phys. Chem. B.* 101:782–791.

Chung, L. A. D., J. Lead, and W. F. DeGrado. 1992. Fluorescence studies of the secondary structure and orientation of a model ion channel peptide in phospholipid vesicles. *Biochemistry.* 31:6608–6616.

Cornell, W. D., P. Cieplak, C. I. Bayly, and P. A. Kollman. 1993. Application of RESP charges to calculate conformational energies, hydrogen bond energies and free energy of solvation. *J. Am. Chem. Soc.* 115:9620–9631.

Cornut, I., B. Desbat, M. J. Turlet, and J. Dufourcq. 1996. In situ study by polarization modulated Fourier transform infrared spectroscopy of the structure and orientation of lipids and amphipathic peptides at the air-water interface. *Biophys. J.* 70:305–312.

Damodaran, K. V., K. M. Merz, and B. P. Gaber. 1995. Interaction of small peptides with lipid bilayers. *Biophys. J.* 69:1299–1308.

de Vocht, M. L., K. Scholtmeijer, E. W. van der Vegte, O. M. H. de Vries, N. Sonveaux, H. A. B. Wösten, J.-M. Ruysschaert, G. Hadziioannou, J. G. H. Wessels, and G. T. Robillard. 1998. Structural characterization of the hydrophobin SC3, as a monomer and after self-assembly at hydrophobic/hydrophilic interfaces. *Biophys. J.* 74:2059–2068.

DeGrado, W. F., and J. D. Lear. 1985. Induction of peptide conformation at apolar/water interfaces: a study with model peptides of defined hydrophobic periodicity. *J. Am. Chem. Soc.* 107:7684–7689.

Eisenberg, D., R. M. Weiss, and T. C. Terwilliger. 1982. The helical hydrophobic moment: a measure of the amphiphilicity of a helix. *Nature.* 299:371–374.

Feenstra, A. K., B. Hess, and H. J. C. Berendsen. 1999. Improving efficiency of large time-scale molecular dynamics simulations of hydrogen-rich systems. *J. Comp. Chem.* 20:786–798.

Ishiguro, R., N. Kimura, and S. Takahashi. 1993. Orientation of fusion-active synthetic peptides in phospholipid bilayers: determination by Fourier transform infrared spectroscopy. *Biochemistry.* 32:9792–9797.

Jacobs, R. E., and S. H. White. 1989. The nature of the hydrophobic binding of small peptides at the bilayer interface: implications for the insertion of transbilayer helices. *Biochemistry.* 28:3421–3437.

Johnson, J. E., N. M. Rao, S. W. Hui, and R. B. Cornell. 1998. Conformation and lipid binding properties of four peptides derived from the membrane-binding domain of CFP: phosphocholine cytidylifransferase. *Biochemistry.* 37:9509–9519.

Kabsch, W., and C. Sander. 1983. Dictionary of protein secondary structure: pattern recognition of hydrogen-bonded and geometrical features. *Biopolymers.* 22:2577–2637.

Kaiser, E. T. and F. J. Kezdy. 1987. Peptides with affinity for membranes. *Annu. Rev. Biophys. Biophys. Chem.* 16:561–581.

Koradi, R., M. Billeter, and K. Wüthrich. 1996. MOLMOL: a program for display and analysis of macromolecular structures. *J. Mol. Graphics.* 14:51–55.

Langmuir, I. 1933. Oil lenses on water and the nature of monomolecular expanded films. *J. Chem. Phys.* 1:756–776.

Lear, J. D., J. P. Schneider, P. K. Kienker, and W. F. DeGrado. 1997. Electrostatic effect on ion selectivity and rectification in designed ion channel peptides. *J. Am. Chem. Soc.* 119:3212–3217.

Mackay, J. P., J. M. Matthews, R. D. Winefield, L. G. Mackay, R. G. Haverkamp, and M. D. Templeton. 2001. The hydrophobin EAS is largely unstructured in solution and functions by forming amyloid-like structures. *Structure.* 9:83–91.

Miyamoto, S. and P. A. Kollman. 1992. SETTLE: an analytical version of the SHAKE and RATTLE algorithms for rigid water models. *J. Comp. Chem.* 13:952–962.

North, C. and D. S. Cafiso. 1997. Contrasting membrane localization and behavior of halogenated cyclobutanes that follow or violate the Meyer-Overton hypothesis of general anesthetic potency. *Biophys. J.* 72:1754–1761.

Pérez-Payá, E., J. Dufourcq, L. Braco, and C. Abad. 1997. Structural characterisation of the natural membrane-bound state of melittin: a fluorescence study of dansylated analogue. *Biochim. Biophys. Acta.* 1329:223–236.

Pohorille, A. and M. A. Wilson. 1993. Isomerization reactions at aqueous interfaces. *In Proceedings on the 26 Jerusalem Symposium on Quantum Chemistry and Biochemistry, Reaction Dynamics in Clusters and Condensed Phases.* B. Pullman and R. D. Levine, editors, Vol. 26. Kluwer, Dordrecht, The Netherlands 207–226.

Pohorille, A. and M. A. Wilson. 1994. Interaction of a model peptide with a water-bilayer system. *In Structure and Reactivity in Aqueous Solution: Characterization of Chemical and Biological Systems.* C. J. Cramer and D. G. Truhlar, editors. ACS Symposium Series No. 568. ACS, Washington, DC. 395–408.

Pohorille, A. and M. A. Wilson. 1996. Excess chemical potential of small solutes across water-membrane and water-hexane interfaces. *J. Chem. Phys.* 104:3760–3773.

Pohorille, A., M. A. Wilson, and C. Chipot. 1997. Interaction of alcohols and anesthetics with the water-hexane interface: a molecular dynamics study. *Prog. Colloid Polym. Sci.* 103:29–40.

Russell, C. J., D. S. King, T. E. Thorgeirsson, and Y. K. Shin. 1998. De novo design of a peptide which partitions between water and phospholipid bilayers as a monomeric α-helix. *Prot. Eng.* 11:539–547.

Ryckaert, J. P., G. Ciccotti, and H. J. C. Berendsen. 1977. Numerical integration of the cartesian equations of motion of a system with constraints; molecular dynamics of *n*-alkanes. *J. Comp. Phys.* 23:327–341.

Schladitz, C., E. P. Vieira, H. Hermel, and H. Möhwald. 1999. Amyloid-β-sheet formation at the air-water interface. *Biophys. J.* 77:3305–3310.

Schuler, L. and W. F. van Gunsteren. 2000. On the choice of dihedral angle potential energy functions for n-alkanes. *Mol. Sim.* 25:301–319.

Segrest, J. P., D. W. Garber, C. G. Brouillette, S. C. Harvey, and G. M. Anantharamaiah. 1994. The amphipathic α-helix: a multifunctional

structural motif in plasma apolipoproteins. *Adv. Prot. Chem.* 45: 303–369.

Stenhagen, E. 1955. Surface films. *In Determination of Organic Structures by Physical Methods.* E. A. Braude and F. C. Nachod, editors. Vol. 1. Academic Press Inc, New York, NY. 325–371.

Takahashi, S. 1990. Conformation of membrane fusion-active 20-residue peptides with or without lipid bilayers: implication of α-helix formation for membrane fusion. *Biochemistry,* 29:6257–6264.

Talbot, N. J., M. J. Kershaw, G. E. Wakley, O. M. H. de Vries, J. G. H. Wessels, and J. E. Hamer. 1996. MPG1 encodes a fungal hydrophobin involved in surface interactions during infection-related developement of *Magnaporthe grisea. Plant Cell.* 8:985–999.

Tamm, L. K., J. M. Tomich, and M. H. Saier. 1989. Membrane incorporation and induction of secondary structure of synthetic peptides corresponding to the N-terminal signal sequences of the glucitol and mannitol permeases of *Escherichia coli. J. Biol. Chem.* 264:2587–2592.

van der Spoel, D., B. Hess, K. A. Feenstra, E. Lindahl, and H. J. C. Berendsen. 1999. *GROMACS User Manual version 2.0.* Nijenborgh 4, 9747 AG Groningen, The Netherlands. Internet: http://md.chem.rug.nl/ ∼gmx.

van Gunsteren, W. F., S. R. Billeter, A. A. Eising, P. H. Hünenberger, P. Krüger, A. E. Mark, W. R. P. Scott, and I. G. Tironi. 1996. *Biomolecular Simulation: GROMOS96 Manual and User Guide.* BIOMOS b.v., Zürich, Groningen.

Voglino, L., T. J. McIntosh, and S. A. Simon. 1998. Modulation of the binding of signal peptides to lipid bilayers by dipoles near the hydrocarbon-water interface. *Biochemistry.* 37:12241–12252.

Vriend, G. 1990. WHAT IF: a molecular modeling and drug design program. *J. Mol. Graph.* 8:52–56.

Wessels, J. G. H. 1994. Developmental regulation of fungal cell wall information. *Annu. Rev. Phytopathol.* 32:413–437.

Wessels, J. G. H. 1997. Hydrophobins, proteins that change the nature of fungal surface. *Adv. Microb. Physiol.* 38:1–45.

Wessels, J. G. H., O. M. H. de Vries, S. A. Ásgeirsdòttir, and F. H. J. Schuren. 1991. Hydrophobins genes involved in formation of aerial hyphae and fruit bodies in *Schizophyllum commune. Plant Cell.* 3:793–799.

Wolfenden, R., L. Andersson, P. M. Cullis, and C. C. B. Southgate. 1981. Affinities of amino acid side chains for solvent water. *Biochemistry.* 20:849–855.

Wösten, H. A. B., O. M. H. de Vries, and J. G. H. Wessels. 1993. Interfacial self-assembly of a fungal hydrophobin into a hydrophobic rodlet layer. *Plant Cell.* 5:1567–1574.

Wösten, H. A. B., F. H. J. Schuren, and J. G. H. Wessels. 1994. Interfacial self-assembly of a hydrophobin into an amphipathic protein membrane mediates fungal attachment to hydrophobic surfaces. *EMBO J.* 13: 5848–5854.

Wösten, H. A. B., and J. G. H. Wessels. 1997. Hydrophobins from molecular structure to multiple functions in fungal development. *Mycoscience.* 38:363–374.

Wu, Y., K. He, S. J. Ludtke, and H. W. Huang. 1995. X-ray diffraction study of lipid bilayer membranes interacting with amphiphilic helical peptides: diphytanoyl phosphatidylcholine with alamethicin at low concentrations. *Biophys. J.* 68:2361–2369.

Xu, Y., and P. Tang. 1997. Amphiphilic sites for general anesthetic action? evidence from [129]Xe-{[1]H} intermolecular nuclear overhauser effects. *Biochim, Biophys. Acta,* 1323:154–162.